AERODYNAMIC ASSESSMENT OF LATERAL JET SHEETS AND THEIR INFLUENCE ON WING-BODY COMBINATIONS FOR SOME BLOWING ARRANGEMENTS

Mihai Neamtu, *Dr. Eng.*
INCAS (Institutul National de Cercetari Aerospatiale "Elie Carafoli"), **Bucharest, Romania**.

Abstract

In this paper the aerodynamic model of the lateral jet sheet and corresponding mathematical relations are presented in a shape useful for aerodynamic interference investigations. The mathematical relations describing the jet sheet are matched in a general computation method for non planar lifting systems, capable to solve the aerodynamic interference problem for a general wing-body configuration and lateral blowing arrangements. Computed results for wing- and body-wing configurations with inclined lateral jets, for different incidences, maximum lift capacities of wing sections or lateral blowing inclinations are presented. The theoretical results are compared with experimental data in the case of rectangular wing with lateral jets. A discussion of the overall aerodynamic effect of different contributions taken into account for the jet sheet modeling is presented. Also, a new manner of using lateral jets, by blowing out of the fuselage in front of the wing, as a fluid close coupled canard, is shortly discussed in connection with an experimental program in development at INCAS.

Introduction

E. Carafoli[1] first reported, in 1962, on the influence of lateral blowing from the tips of rectangular wings on their lifting characteristics. Since then, a number of studies have been performed in Romania (at the Institute for Fluid Mechanics in Bucharest), or other countries[7-8]. Regarding the Romanian research, although the essential theoretical or experimental developments were communicated in different publications[2-5], others, containing, important developments, remained only in the shape of basic research reports and in the present paper author's Ph.D. thesis[6], unfortunately having a rather reduced circulation. This was one of the reasons for allocating a good part of this paper to summarise some of the practically unpublished results contained in [6].

On the other hand, recent developments renewed the interest for the entire problem, especially in connection with the idea of using the lateral jet sheets as *canard-like fluid surfaces, close-interacting with the wing as vortex lift generators*, in addition to the direct effect on the body. Experimental results are not yet available, but a wind-tunnel experimental program is scheduled to start in the summer of this year.

The aerodynamic model of the lateral jet sheet is developed in the framework of a lifting surface theory, specially build to allow a separate treatment of the chordwise problem and the reduction of the spanwise problem to a modified lifting line method that is accurate for all aspect ratios and suitable for non-planar lifting systems.

Theoretical background

The jet sheet model

Consider a thin jet sheet exiting y-wise, as in Fig. 1, trough a wing tip slot of chord c_0 and thickness δ_j. Let V_j and U_∞ be the jet and main flow velocities and ρ_j and ρ_∞ the corresponding air densities. The jet momentum rate and the associated jet coefficient are given by the following formula:

$$J = \rho_j \delta_j c_0 V_j^2 \; ; \qquad C_j = \frac{2J}{\rho_\infty U_\infty^2 c_0^2} \tag{1}$$

For the sake of simplicity, unless otherwise specified, the slot camberline will be neglected and the jet momentum considered to be uniformly distributed along the slot.

Preparatory analyse and assumptions. In order to obtain a correct representation of a lateral jet sheet we have to analyse the different types of its interactions with the main flow.

The firsts to be discussed are the viscous interactions for which a hypothetical non lifting case was considered. The main phenomenon is the entraining of the two flows one in the direction of the other, as sketched in Fig. 2. The initial thin jet sheet is replaced, as departing from the exit slot, by a core of particles having velocity components both in the jet and main flow directions. This core increases on the expense of the main flow particles entrained by the jet. A two direction momentum analysis, performed in [6], produced the following formula for the average sweep angle Λ of the jet core:

$$\tan\Lambda = [\frac{Q(y)}{Q_0} - 1]\frac{U_\infty}{V_j} + \text{order}(\frac{U_\infty^2}{V_j^2}) + \ldots \tag{2}$$

...where $Q(y)$ and Q_0 are the flow rates in the jet core at a current station y and at the slot, respectively.

As one can see no matter how small is $\frac{U_\infty}{V_j}$ the sweep angle tangent, tanΛ, increases indefinitely with y because of the entrainment effect included in Q(y).

On the other hand, for $V_j >> U_\infty$ there is a certain neighbourhood of the slot where the sweep angle can be considered small enough to be neglected, together with the entrainment effects.

The second type of interactions to be considered are those due to the potential flow around the jet core, mainly the lifting interactions. These interactions are the most important for the purposes of this paper and will be treated in detail.

Confining the analyse to the region in the neighbourhood of the slot and to the case $V_j >> U_\infty$ the following assumptions can be made [Carafoli [1,2]]:

-The jet sheet behaves like a solid deforming lifting surface (*the concept of the equivalent fluid wing*);

-It can be decomposed into elementary thin jet filaments that preserve their slot momentum magnitude (δJ) while changing their direction under the pressure differences acting between the lower and upper side of the jet sheet (*the concept of the jet filaments*).

A third assumption, based on the momentum theorem, is essential to establish a termination criterion for the lifting part of the jet sheet, which in turn defines the span or the planform of the equivalent fluid wing:

-The overall lift supported by the equivalent wing representing the jet sheet, P_j, equals in magnitude the jet momentum at the slot:.

$$J = P_j \qquad (3)$$

This assumption was one of the contributions introduced by the present author in [3]. It was used in all subsequent works [Carafoli and Neamtu [3,4,5], Neamtu [6]].

It can be easily extended to the case of the jet sheets having a slotwise variation of the direction of jet exit velocity, if we use instead of J the sum of the momentum magnitudes of all jet filaments, ΣδJ. The physical meaning is that the jet sheet terminates along a line where the jet filaments have a direction perpendicular to the total slot momentum **J**, considered as a vectorial resultant (in general $\Sigma\delta J \geq |\mathbf{J}|$).

The above assumptions allow a variety of aerodynamic models for the equivalent wing. Two extreme models are shown in Figure 3.

Model I represents a plane equivalent wing for which the leading edge filaments are immediately deformed and rotated with 90°, producing, possibly, a chord variation. This type of model can be associated with pressure difference distributions featuring a pronounced peak at the leading edge, as in the case of very small aspect ratio wings.

Model II is the most general and assumes a more gradual chordwise pressure distribution, resulting in a non-planar shape of the equivalent wing (twisted and bent).

In the following the general model II will be considered, but a discussion will be made at the end of the paper about the differences obtained by using various models for the equivalent wing.

Deformation relations. All the relations defining the equivalent wing correspond to the properties of the jet sheet in the vicinity of the slot that are assumed to extend up to the wing tip. The usual small perturbation approximations apply nearly to the entire wing *because of the abrupt rolling up of the jet filaments in the region of jet sheet termination.*

The jet filaments (as defined above) bend under the action of pressure differences Δp. Applying the momentum theorem the deviation angle β and the ordinate z(y) of the deformed jet filament can be written as follows:

$$\sin\beta = \frac{\partial z}{\partial y}\cos\beta = \frac{1}{c_0 C_j}\int_0^y \Delta C_p dy' \qquad (4)$$

$$z = \frac{1}{c_0 C_j}\int_0^y \frac{\int_0^{y'} \Delta C_p dy''}{\cos\beta} dy' \cong \frac{1}{c_0 C_j}\int_0^y \left(\int_0^{y'} \Delta C_p dy''\right) dy' \qquad (5)$$

...where $\Delta C_p = 2\Delta p / \rho_\infty U_\infty^2$

From the above formula one can extract the equations defining a mean deformation line by averaging along the chord:

$$\sin\beta_m = \frac{1}{c_0 C_j}\int_0^y C_l dy' \cong \tan\beta_m \qquad (6)$$

$$z_m = \frac{1}{c_0}\int_0^{c_0} z dx \cong \frac{1}{c_0 C_j}\int_0^y \left(\int_0^{y'} C_l dy''\right) dy' \qquad (7)$$

...where $C_l(y) = \frac{1}{c_0}\int_0^{c_0} \Delta C_p(x,y) dx$ is the sectional lift coefficient.

Also, one can derive an approximate expression of the geometrical incidence $\alpha_n(x,y)$ defined in a plane *normal* to the jet sheet

$$\alpha_{nj}(x,y) = \frac{w_n(x,y)}{U_\infty} \cong \alpha_0 \cos[\beta_m(y) - \varphi_0] - \frac{1}{c_0 C_j}\int_0^y \left(\int_0^{y'} \frac{\partial \Delta C_p(x,y)}{\partial x} dy''\right) dy' \qquad (8)$$

where $w_n(x,y)$ is the component of U_∞ normal to the jet surface, while α_0 and φ_0 are the incidence of the slot and the jet lateral inclination, respectively.

Aerodynamic analysis. The relations above express the deformations of the jet sheet as a function of the pressure differences resulting from the aerodynamic interactions with the main flow. These interactions depend, in turn, on the incidence and geometry of the entire lifting system, including the jet portions, and can be expressed in the framework of the lifting surface theory. In the previous works [3-6] the downwash equation of the lifting surface (in

fact the boundary condition in terms of downwash induced by the vortex system that model the lifting surface) was written in the following shape:

$$\alpha_n(x,y) = i_n(y) + \frac{\psi}{4\pi}\int_0^c \frac{\Delta C_p(x_0,y)}{x_0 - x}dx_0 \qquad (9)$$

...where $i_n(y)$ is *the sectional induced incidence in the sense defined by Prandtl* and ψ is a correction coefficient to allow for low aspect ratio effects. For ψ=1 the above equation is exactly the equation of the lifting surface for the limiting case of infinite aspect ratio and the last term coincides with Birnbaum's expression for the downwash induced by the infinite spanwise bound vortices. As shown in [6] Eq. (9) can be used for nonplanar unswept lifting surfaces of low aspect ratio, with ψ given by the following theoretically derived expression:

$$\psi = \sqrt{1 + \frac{4\kappa^2}{A^2}} = \sqrt{1 + \frac{2}{A^2}} \qquad (10)$$

This takes into account the influence of the aspect ratio A, κ being a constant, whose value, corresponding to $4\kappa^2$=2, was found in a way that will be explained below.

This time the last term in (9) represents the downwash induced not only by the spanwise bound vortices (as in Birnbaum's case) but also by all segments of streamwise vortices overlooked or added in the $i_n(y)$ computation.

Following a known way, multiplying Eq. (9) by $\sqrt{(c-x')/x'}$ and integrating along the chord for x' from 0 to c, one finally obtains:

$$C_l(y) = \frac{2\pi}{\psi(A)}[(\alpha^*(y) - i_n(y)] \qquad (11)$$

...where $C_l(y)$, as above, is the section lift coefficient, accounting for $\frac{1}{c}\int_0^c \Delta C_p(x',y)dx'$, while $\alpha^*(y)$ is the section geometric incidence considered from the zero lift axis of the section and represents the expression $\frac{2}{\pi c}\int_0^c \sqrt{\frac{c-x}{x}}\alpha(x',y)dx'$.

Eq. (11) is similar to Prandtl's lifting line equation, differing only by the factor $1/\psi$. By using this equation one can determine the variation with the aspect ratio A of the total lift coefficient C_L of rectangular wings. By simply comparing with the experimental results, one finds the value $4\kappa^2$=2, that appears in the expression (10) of ψ.

Eq. (11) also defines a slope "a" of the local lift coefficient C_l corresponding to an effective incidence $\alpha_e=\alpha^*-i_n$

$$a = \frac{2\pi}{\psi} = \frac{2\pi}{\sqrt{1 + 2/A^2}} \qquad (12)$$

Both a and α_e differ from the apparently similar notions introduced by Kücheman in [9] because i_n is defined in a different manner.

The nonplanar lifting surface to which Eq. (9) applies is of a quasi-cylindrical shape, together with the vortex wake behind it. Its spanwise configuration can be defined by the trace in the Trefftz plane far behind the lifting surface itself.

Turning now to the jet sheet and taking into account the deformation relations, by applying (9) one obtains the jet sheet equation:

$$\alpha_0\cos[\beta_m(y) - \varphi_0] - \frac{1}{c_0 C_j}\int_0^y\left(\int_0^{y'}\frac{\partial\Delta C_p(x,y)}{\partial x}dy''\right)dy' =$$

$$= i_n(y) + \frac{\psi}{4\pi}\int_0^c \frac{\Delta C_p(x_0,y)}{x_0 - x}dx_0 \qquad (13)$$

The main advantage of using Eq. (9) and consequently (13) consists in the separation of the chordwise and spanwise interactions. This allows to treat first the chordwise problem and establish the equivalent sectional geometric incidence that, in turn, can be used to treat the spanwise problem, in the framework of the lifting line Eq. (11).

The procedure, based on the classical chordwise development of $\Delta C_p(x,y)$ in a Glauert shape (however with coefficients depending on y), was used in [3,4,5,6] and resulted in the following expression of sectional incidence corresponding to the local zero lift axis:

$$\alpha^*_{nj}(y) \cong \alpha_0\cos[\beta_m(y) - \varphi_0] + \alpha_j(y) \qquad (14)$$

...where:

$$\alpha_j(y) \cong \frac{8/(\pi\sqrt{2})}{c_0 C_j}\int_0^y\left(\int_0^{y'} C_l dy''\right)dy' \qquad (14')$$

In [6] the procedure was also extended to find the 2-D shape of the jet sheet, for the case C_l=constant.

The equivalent wing (model II) of the jet sheet. We can now define the equivalent wing by extending, with some special precautions, the relations established for the region in the vicinity of the exhaust slot to the extremity of the jet. This can be done , following [6], as follows:

-constant chord ($c=c_0$)

-The shape of the lifting line will be given by the relations (6) and (7). However in (6) the approximate part will be considered, in order to be consistent with the approximation in (7). This means that β_m will be taken as:

$$\beta_m \cong a\tan\left(\frac{1}{c_0 C_j}\int_0^y C_l dy'\right) \qquad (15)$$

-The sectional incidence given by the following alternate relation, rather then (14):

$$\alpha^*_{nj}(y) \cong \alpha_0\cos[\beta_m(y) - \varphi_0] + \frac{\alpha_j(y)}{\sqrt{1 + [\alpha_j(y)]^2}} \qquad (16)$$

As one can see for small $\alpha_j(y)$ the above relation tends to the expression (14).

-According to the termination condition (3), the span of the equivalent wing will be implicit in the following equation, as the upper limit of the integral:

$$c_0^2 C_j = \chi c \int_0^{b_j} C_l dy' \qquad (17)$$

...where χ is a parameter close to 1, that can be used for a final empirical adjustment.

Lifting systems with inclined lateral jets

Consider a lifting system having in the Trefftz plane a trace as in Fig. 4 and let s be a scalar spanwise coordinate chosen in a convenient manner, as will be explained bellow.

Introducing the circulation Γ instead of the section lift coefficient C_l , ($2\Gamma = cU_\infty C_l$), and using s instead of y, the induced incidence in equation (11) can be expressed as follows:

$$i_n(s) = \frac{1}{4\pi U_\infty} \int_{-s_B}^{s_B} \frac{\Gamma(s') \cdot g(s,s',\Gamma)}{(s-s')^2} ds' \qquad (18)$$

...where g(s,s',Γ) is an "interference" function that takes into account the non-planar effects, including the presence of the fuselage and the Γ-dependent jet portions of the trace.

In the above relation and in all relations below, containing a kerner of the same type as $[(s-s')^2]^{-1}$, the integral represents the second-order principal value in Mangler's sense.

As a consequence the lifting line equation (11) can be rewritten in the following form:

$$\Gamma(s) = \frac{\pi c U_\infty}{\psi(A)} [\alpha^*(s,\Gamma) - \frac{1}{4\pi U_\infty} \int_{-s_B}^{s_B} \frac{\Gamma(s') \cdot g(s,s',\Gamma)}{(s-s')^2} ds'] \qquad (19)$$

In the following, for the sake of simplicity, only symmetrical systems will be considered.

The limits of the above integrals result from the termination condition Eq. (17).

The general procedure. Because of the complex inter-dependence between the shape of the configuration in the Trefftz plane and the spanwise circulation distribution, an iterative procedure is required to solve the integro-differential equation (19), as follows:

Step 1.-Chose the length of the jet sheets, b_j and hence s_B;

Step 2.-For the first iteration, establish the configuration by using independent on Γ simplified formula defining the lifting line geometry (z_m and β_m) and sectional incidence (α_j) for the jet portions (see below);

Step 3-Calculate $\alpha^*_{nj}(s)$, using (16), and g(s,s') (see below) for the resulting configuration;

Step 4.-Compute the circulation distribution (see method below);

Step 5.-Recalculate z_m, β_m and α_m by using this time the normal relations;

Step 6-Repeat from step 3 until the difference between two successive iterations becomes negligible.

Step 7-Calculate C_j and the overall aerodynamic coefficients of the solid part of lifting system.

Normal and simplified expressions for z_m, β_m and α_m. The following relations are written, for the simplicity sake, in the Oxyz system of the jet sheet, using Γ instead of C_l and taking into account (17):

$$\beta_m \cong a\tan\left(\frac{1}{\chi} \frac{\int_0^y \Gamma dy'}{\int_0^{b_j} \Gamma dy'}\right) \cong a\tan\left(\frac{1}{\chi} \frac{y}{b_j}\right) \qquad (20)$$

$$z_m(y) \cong \frac{\int_0^y (\int_0^{y'} \Gamma dy'') dy'}{\chi c_0 \int_0^{b_j} \Gamma dy'} \cong \frac{0.5}{\chi} \cdot \frac{b_j}{c_0} \cdot \left(\frac{y}{b_j}\right)^2 \qquad (21)$$

$$\alpha_j(y) \cong \frac{8}{\pi\sqrt{2}} \frac{\int_0^y (\int_0^{y'} \Gamma dy'') dy'}{\chi c_0 \int_0^{b_j} \Gamma dy'} \cong \frac{0.8925}{\chi} \cdot \frac{b_j}{c_0} \cdot \left(\frac{y}{b_j}\right)^2 \qquad (22)$$

The numerical method for Eq.(19). The Multhopp method [see for example [10]] allows the determination of the adimensional circulation, hereto defined by:

$$\gamma = \frac{\Gamma}{2 s_B U_\infty} = \frac{c C_l}{4 s_B} \qquad (23)$$

...for (2N-1) stations along the span of nonplanar wing:

$$s_\nu = s_B \cos\left(\frac{\nu\pi}{2N}\right), \quad \nu = 1,2,....(2N-1) \qquad (24)$$

In the general case, Eq.(19) transforms into a system of (2N-1) linear equations for the values of γ_ν corresponding to the stations (24). However, for the symmetrical case considered here, only N equations are necessary.

$$\gamma_\nu \left(G_{\nu\nu} + \frac{4 s_B}{a_\nu c_\nu}\right) + \sum_{\mu=1}^{N} \gamma_\mu \bar{G}_{\nu\mu} = \alpha^*_\nu \qquad (25)$$

...where: $\nu = 1,2,....N$

$$\bar{G}_{\nu\mu} = b_{\nu\mu} G_{\nu\mu} + b_{\nu,2N-\mu} G_{\nu,2N-\mu}, \quad \nu \neq \mu \qquad (25')$$

$$\alpha_\nu = \alpha^*(s_\nu) \qquad (26)$$

$$G_{\nu\nu} = b_{\nu\nu} g_{\nu\nu} = \frac{N}{2\sin(\frac{\nu\pi}{2N})} g_{\nu\nu} \qquad (27')$$

$$G_{\nu\mu} = b_{\nu\mu} g_{\nu\mu} =$$

$$= -\frac{1+(-1)^{\nu-\mu}}{4N} \frac{\sin(\frac{\nu\pi}{2N})}{[\cos(\frac{\nu\pi}{2N}) - \cos(\frac{\mu\pi}{2N})]} g_{\nu\mu} \qquad (27'')$$

$$g_{\nu\mu} \overset{def}{=} \lim_{s' \to s_\mu} g(s_\nu, s') \qquad (28)$$

The expressions for $g(s_\nu,s')$ will be presented below

The body-wing-inclined lateral jets configuration Refer to Fig. 4 and consider the complex plane $\zeta\Omega\eta$, with $\Omega\eta$ as imaginary axis and $t=\zeta+i\eta$ the associated complex variable. Denote by D the trace of the wing, interrupted by the fuselage in F and $\bar{F}$ and let M be a point on D while M_y represents its orthogonal projection on the known trace FOB_y (with B_y and B corresponding in the same manner as M_y and M). On the solid portion $M \equiv M_y$.

Also let σ be the length of the portion FM_y , measured on the trace FOB_y . The coordinate s, corresponding to M and M_y can be defined as $s=s(\sigma)$, where $s(\sigma)$ can be chosen in a manner that produce a favourable distribution of the points σ_ν corresponding to the stations in (23), by increasing their density in the regions of rapid variation of $\gamma(s)$, $\alpha^*(s)$, or $g(s,s')$. We denote by σ_o ,s_o, σ_B, s_B the values of σ and s corresponding to O and B, respectively.

The configuration of the lifting system can easily be described by using the complex variable $t=\zeta+i\eta$. For a point M on the jet portion, corresponding to M_y on Oy, one can write:

$$t(M) = t(M_y) - z_m(y) e^{-i\varphi_o}; \qquad (29')$$

$$\frac{dt}{d\sigma} = \frac{e^{i\varphi}}{\cos\beta_m(y)}$$

where $\varphi=\mathrm{Arg}(dt/d\sigma)$ and

$$t(M_y) = t(O) + y \cdot ie^{-i\varphi_o} =$$

$$= t(s_O) + [\sigma(M_y) - \sigma_o)] \cdot ie^{-i\varphi_o}$$

For the solid portion $t(M)=t[s(\sigma)]$ must correspond to the given configuration and position of the solid wing. For a horizontal wing passing through Ω one can write

$$t=t_F+(t_0-t_F)\cdot\sigma(s)/\sigma_o \qquad (29'')$$

We notice that φ_o represents the jet lateral inclination at the slot, corresponding (see Fig. 4) to $(\pi/2-\varphi)$ in O (but on the jet side only).

Following Multhopp's method for wing-body combinations[11], [12] , the plane $\zeta\Omega\eta$ is conformally mapped on a plane ζ^* with the fuselage superposed on the $\Omega^*\eta^*$ axis, as in Fig. 4.

There are two effects of the fuselage that have to be accounted for:

-the modification of the downwash induced by the vortex wake, or, in other words, of the induced incidence;

-the alteration of the incident flow, i. e. of the attack incidence of the main flow.

Lets treat first the induced downwash, starting with the flow in the Treffz plane, far behind the real system.

As known, the conformal mapping does not change the potential of the plane flow and so Γ remains also unchanged. In the transformed plane, the complex velocity due to Γ in a point M^* on the transformed trace D^*, corresponding to M on the trace D in the Trefftz plane, is given by:

$$\overline{w_\infty^*} = \frac{i}{2\pi} \int_{D^*} \frac{d\Gamma'}{(t^* - t^{*\prime})} = -\frac{i}{2\pi} \int_{D^*} \frac{\Gamma' dt^{*\prime}}{(t^* - t^{*\prime})^2} \qquad (30)$$

The complex velocity in M, on the trace D in the Trefftz plane is

$$\overline{w_\infty} = \overline{w_\infty^*} \left(\frac{dt^*}{dt}\right) \qquad (31)$$

The component of the real velocity w_∞ , normal in M to the trace D is given by

$$w_{n\infty} = \mathrm{Re}(-ie^{i\varphi}\overline{w_\infty}) \qquad (32)$$

(Note:The above relation contains also a general procedure to obtain in a simple manner the component of the velocity normal to the lifting line trace starting from the corresponding complex velocity.)

Taking into account (30) to (32) the incidence induced normal to the *real* lifting line in the point corresponding to M on D, can be written in the following shape:

$$i_n = \frac{w_{n\infty}}{2U_\infty} = -\frac{1}{4\pi U_\infty} \mathrm{Re}\left[e^{i\varphi} \frac{dt^*}{dt} \int_D \frac{\Gamma'(\frac{dt^*}{dt})' dt'}{(t^* - t^{*\prime})^2} \right] \qquad (33)$$

$$= \frac{-1}{4\pi U_\infty} \int_D \frac{\Gamma \cdot \mathrm{Re}\left[\frac{(s-s')^2}{(t^* - t^{*\prime})^2} \frac{dt^*}{dt} \frac{dt^{*\prime}}{dt'} \frac{dt'}{d\sigma'} \frac{d\sigma'}{ds'} e^{i\varphi} \right]}{(s-s')^2} ds'$$

Comparing the last part of the above relation with (18), one can easily see that:

$$g(s,s',\Gamma) = \mathrm{Re}\left[\frac{(s-s')^2}{(t^* - t^{*\prime})^2} \frac{dt^*}{dt} \frac{dt^{*\prime}}{dt'} \frac{dt'}{d\sigma'} \frac{d\sigma'}{ds'} e^{i\varphi} \right] \qquad (34)$$

Now, taking into account (28)and (29) one obtains, after some simple handling:

$$G_{\nu\nu} = b_{\nu\nu} g_{\nu\nu} = \frac{N}{2} \frac{\cos\beta_{m\nu}}{\sin(\frac{\nu\pi}{2N}) \cdot (\frac{d\sigma}{ds})_\nu} \qquad (35)$$

$$G_{\nu\mu} = -\frac{[1+(-1)^{\nu-\mu}]}{4} G_{\mu\mu} \mathrm{Re}\left[\frac{(\frac{dt^*}{dt})_\nu (\frac{dt^*}{dt})_\mu}{(t_\nu^* - t_\mu^*)^2} e^{i(\varphi_\nu + \varphi_\mu)} \right]$$

The calculus of $\overline{G}_{\nu\mu}$ in (25) is now only a matter of taking into account the symmetry of the lifting system.

Considering now the effect of the fuselage on the incoming flow and following a known way, it can be written in terms of an additional angle of attack normal to the lifting line:

$$\alpha_{bn} = -\alpha_B \, \mathrm{Re}[ie^{i\varphi}(\frac{dt^*}{dt} - 1)] \qquad (36)$$

...where α_B is the incidence of the body axis.

Further, the total incidence in the right side of (25) can be calculated by adding (36) to the incidences due to the angle of attack or to the shape of the lifting system such as (16) for the jet portions.

The conformal mapping and $s(\sigma)$ for the elliptic or circular cross section fuselage: The following relations are written in a shape that cover both cases:

$$t^* = \frac{(H+L)(t^2+L^2)}{(Ht + L\sqrt{t^2 - H^2 + L^2})} \qquad (37)$$

$$\frac{dt^*}{dt} = \frac{(H+L)(t^2-H^2)}{(Lt + H\sqrt{t^2 - H^2 + L^2})\sqrt{t^2 - H^2 + L^2}} \qquad (38)$$

One chose now the co-ordinate transformation $s(\sigma)$ so as to coincides with the conformal transformation of $\Omega\eta$ axis by putting $t=i(\sigma+L)$ and $t^*=is$

$$s = \frac{(H+L)[(\sigma+L)^2 - L^2]}{H(\sigma+L) + L\sqrt{(\sigma+L)^2 + H^2 - L^2}} \qquad (39)$$

... with the inverse

$$\sigma = \frac{Hs + L\sqrt{s^2 + (H+L)^2}}{(H+L)} - L \qquad (40)$$

...and the derivative:

$$\frac{d\sigma}{ds} = \frac{Ls + H\sqrt{s^2 + (H+L)^2}}{\sqrt{s^2 + (H+L)^2}} \qquad (41)$$

The overall aerodynamic characteristics. Before presenting the expressions of the overall aerodynamic coefficients it is useful to mention an important remark of E. Carafoli[13], regarding the total aerodynamic lift of a wing-body combination:

the lift computed for the trace of the wing in the transformed Trefftz plane equals the total lift of the wing-body combination.

This can be simply understood by noticing that the integrals of the complex potential $F=\Phi+i\Psi$ on the circle at infinity calculated in the Trefftz and in the conformally mapped plane are the same, because the potentials are the same and the deformations due to confomal mapping vanish at infinity. Or, as known, the real part of these integrals multiplied by the imaginary unit i, represents the overall lift of the entire system, so demonstrating the above statement.

As a consequence the total lift of the body can be calculated without knowing its distribution on the fuselage. This can be done by simply subtracting from the above total lift, the lift corresponding to the wing portions, that can be found by integrating along the wing trace in the Trefftz plane. Hence, in terms of complex variables:

$$P_f = \rho_\infty U_\infty \, \mathrm{Re}[i(\int_{D^*} \Gamma dt^* - \int_D \Gamma dt)] =$$

$$= \rho_\infty U_\infty \, \mathrm{Re}[i\int_D (\frac{dt^*}{dt} - 1)\Gamma dt)] \qquad (42)$$

As shown in [6] the repartition of this lift across the fuselage can be found using the same procedure as in [12], but resulting the following formula:

$$P_f(\eta) = \rho_\infty U_\infty \Gamma_F + (2/\pi)[(P_f/(2\eta_F) - \rho_\infty U_\infty \Gamma_F][\zeta_u(\eta) - \zeta_l(\eta)] \qquad (43)$$

...where $\zeta_u(\eta)$ and $\zeta_l(\eta)$ are the upper and lower fuselage ordinates. For the elliptical or circular cross section fuselage $\zeta_u(\eta) - \zeta_l(\eta) = (1-\eta/L)^{1/2}$

The total lift of the solid wing-body combination can be obtained by adding (42) to the lift of the wing alone. The resulting overall wing-body lift coefficient, taking into account (23) is:

$$C_{WB} = \frac{4s_B^2}{S_{WB}} \mathrm{Re}\{i[\int_D \gamma(\frac{dt^*}{dt} - 1)dt' + \int_{t_F}^{t_0} \gamma dt']\} \qquad (44)$$

...where S_{WB} is the surface of the wing, including the portion passing through the body, taken as reference for the entire combination.

As for the induced drag, it can be calculated by spanwise integration of γi_n on the solid wing:

$$C_{Di} = \frac{8s_B}{S_{WB}} \int_0^{\eta_0} \gamma(\alpha^* - \frac{4s_B}{c}\frac{\gamma}{a})d\eta \qquad (45)$$

...where η_0 corresponds to O.

For the jet portion, taking also into account (17), one obtains:

$$C_j = 4\chi \frac{s_B^2}{c_0^2} \int_0^{b_j} \gamma dy' \qquad (46)$$

Results and discussion

The self explanatory Figures 7a,b,c,d show the spanwise circulation distributions for a rectangular wing and for a wing body combination with jets blown outwardly from the tips of the wing. In these figures s, rather then σ, represents the length measured from the fuselage junction along the wing, then along the initial direction of the jet. The results correspond to different incidences of the wing α_w, lateral jet inclinations φ_0 and total length of the jet sheet, $b_j/c_0 = s_B - s_0$. As one can see, by increasing the incidence or the jet length, the lift increases on the entire span but especially in the region close to the jet. By inclining the jets, these features are more pronounced, due

to non-planar effects which are similar with those produced by the winglets.

Figures 8a and b show the increase of the overall lift coefficient due to lateral blowing, for the same incidences as in Fig. 7 and, additionally, for two maximal capacities of the sectional lift coefficient.

The last two situations are defined by considering that the stalling appears when the maximal sectional lift capacity is reached on the wing section in the most central position, far from the jets, as shown in Fig. 5. This corresponds to the assumption that the suction produced by the jets prevents the first appearance of the separation in the sections close to them.

In the case of the rectangular wing of aspect ratio 1.5 with spanwise lateral jets (φ_0=0) the theoretical data are compared with experimental results from [2].

Also shown in Fig. 8 are the lines of constant jet length b_j/c_0 , corresponding to the values considered in Fig. 7.

The calculated induced drag reduction due to lateral blowing is represented in Fig. 9. One can see the important effect of jet inclination.

Figure 10 shows the length of the lateral jet b_j/c_0 for both lifting systems. One notice that the jet inclination and the solid system configuration have a little influence on the jet length. This is valid for any other configurations as shown in [6].

Some interesting remarks can be made about the accuracy of the jet modelling presented in this paper. It is normal to consider that the complex flow around the lateral jet sheet cannot be accurately modelled. To check the influence of the different assumptions, different models were tested and some typical results are presented in Figure 11.

As one can see, the increase of lift due to lateral blowing shows a rather small degree of sensitivity to the type of the model even at high blowing rates (up to 10%). The impression is that this effect can be neglected. This is an important result, that can be helpful especially when looking for approximate formula as in [8]. It means that simple models can produce good approximations of the lift increase due to blowing for a given jet coefficient

However the model type becomes important for the estimation of jet extension, (b_j/c_0), as also one can see in Fig.11, where the errors between the two extreme models amount to more than 50% for C_j=1. In this case the most important effect is introduced by the jet twisting producing the additional jet incidence. The jet bending has a little influence.

The Figure 12 presents the maximum lift gain for different wing and wing-body systems with lateral jets blown spanwisely. the gain coefficient was calculated in % for the condition in fig 5, using the following definition:

$$C_h\% = \left(\frac{C_{LJmax}}{C_{Lmax}} - 1\right)\cdot 100$$

where C_{LJmax} and C_{Lmax} are the maximum lift capacities of the lifting system with and without jets.

An interesting remark is that the blowing appears to be more efficient for wing-body combinations then for wings alone. This result needs an experimental confirmation but from the theoretical point of view it has a simple explanation: the lift on the body is decreased by a quantity, that is proportional with some average downwash in the body region. The decrease starts from the lift level at the wing junction, or, by blowing the downwash decreases while the lift level at the wing fuselage junction increases both effects contributing to a more pronounced lift increase as compared with the case without jets.

Concerning the experiments, a modular model of the shape in Figure 6 is scheduled to be tested this summer in the trisonic wind tunnel of INCAS, as already mentioned. The tests are intended not only for the investigation of wing-body combinations, as considered above, but also for the study of the influence of lateral blowing from the fuselage in front of the wing. Canard like effects are expected to be detected.

References

1. E. Carafoli, *"The influence of Lateral Jets, Simple or Combined with Longitudinal Jets, upon the Wings Lifting Characteristics"*, Proc. of the 3rd ICAS, 1962

2. E. Carafoli, N. Camarasescu, *"Noi cercetãri asupra aripilor de alungire micã cu jeturi laterale"*, Studii si Cercetãri de Mecanicã Aplicatã, XX, 4, 1970. English translation: *"New Researches on Small Span-Chord Ratio Wings with Lateral Jets"*, NTIS, AD-733858.

3. E. Carafoli, M. Neamtu, *"New Theoretical Developments on the Wing with Lateral Jets"*, OMMAGIO A CARLO FERRARI, ed. univ. Levrotto and Bella, Torino, Italia, dec. 1974.

4. E. Carafoli, M. Neamtu, *"Flow around Wings with Inclined Lateral Jets"*, Mech. Research. Comm., vol. 3, no. 3, 1976.

5. E. Carafoli, M. Neamtu, *"Aerodinamica aripilor cu jeturi laterale înclinate"*, Studii si cercetãri de Mecanicã Aplicatã,XXXV, 2, iun. 1976.

6. M. Neamtu, *"Contributii la studiul jeturilor laterale si a aplicatiilor acestora"*, Ph.D. Thesis, 1980.

7. M.M. Briggs and R.G. Schwind, *"Augmentation of Fighter Aircraft Lift and STOL Capability by Blowing Outboard from the tips"*, AIAA-83-0078, AIAA 21st Aerospace Sciences Meeting, 1983, Reno, Nevada.

8. D.A. Tavella et al., *"Lift Modulation with Lateral Wing-Tip Blowing"*, J. of Aircraft, vol.25, no. 4, April 1988.

9. D. Kücheman, A.R.C., R&M 2935, 1952

10.H. Multhopp, A.R.C., R&M 2884, 1950

11.H. Multhopp, *"Aerodynamics of the fuselage"*,A.R.C. 5263, 1941

12. J. Weber, D.A. Kirby, D.J.Kettle, A.R.C., R&M 2872, 1956.

13. E. Carafoli, *Aerodinamica*, 1954. (also, german, russian and chinese versions.

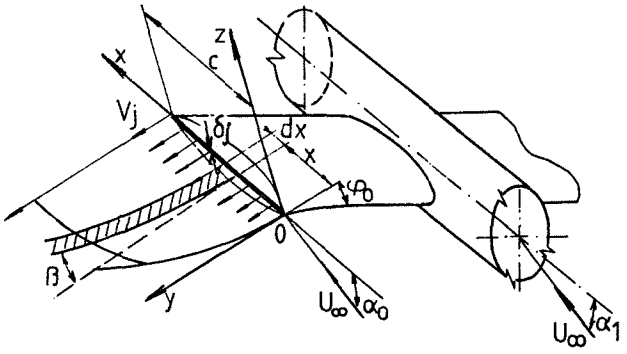

Fig. 1 The body-wing-inclined lateral jets arrangement

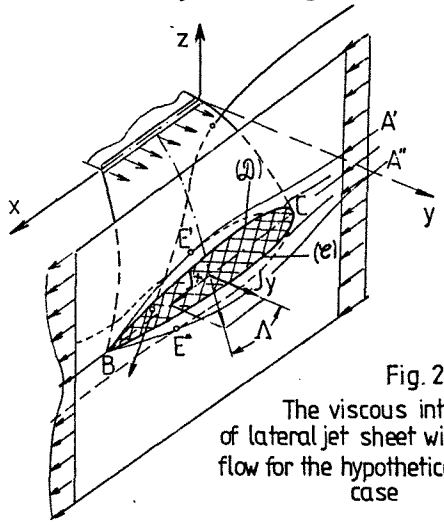

Fig. 2
The viscous interaction of lateral jet sheet with a uniform flow for the hypothetical nonlifting case

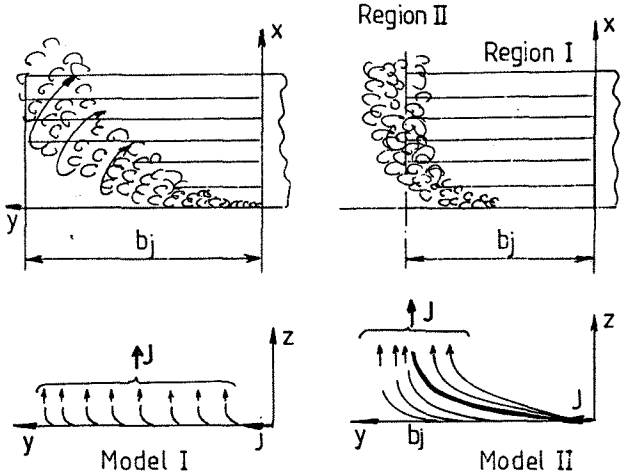

Fig. 3 Two lifting models for the lateral jet sheet

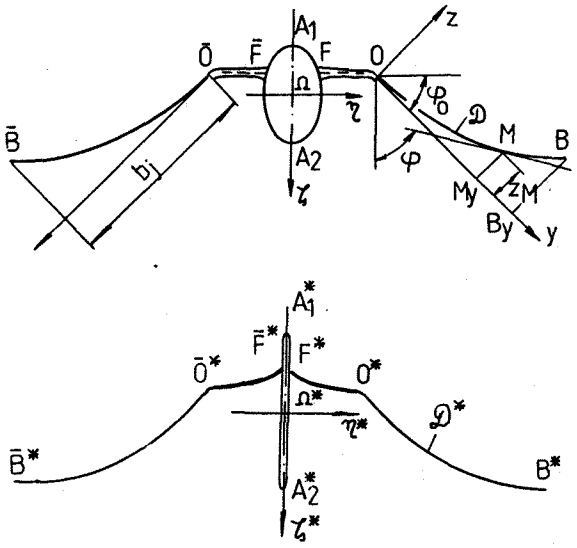

Fig. 4 The configuration of the lifting system in the Trefftz-plane and its conformal mapping

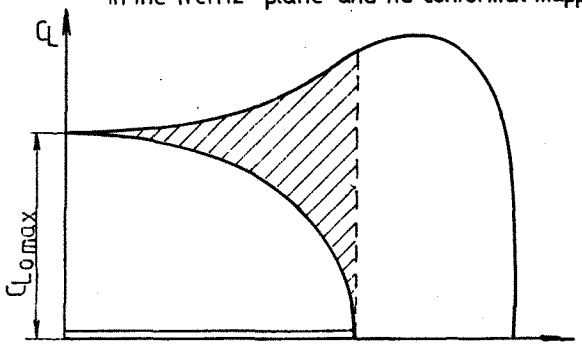

Fig. 5 The maximum increase of the lift due to the influence of the lateral jets

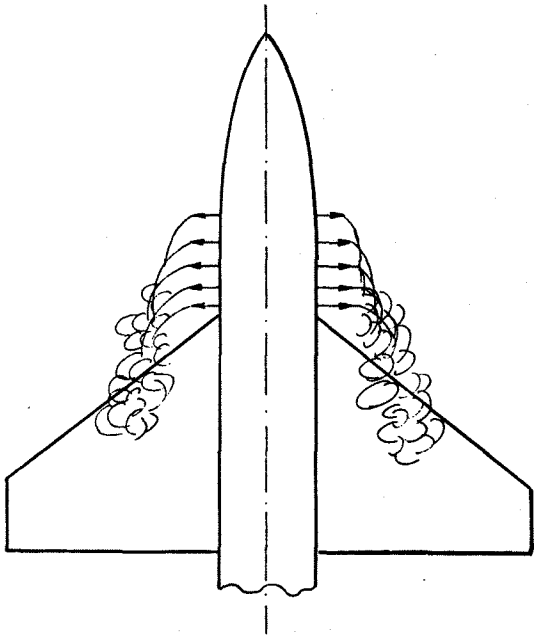

Fig. 6 The body-wing-combination with canard lateral jets

Fig. 7a,b,c,d
Spanwise circulation distributions

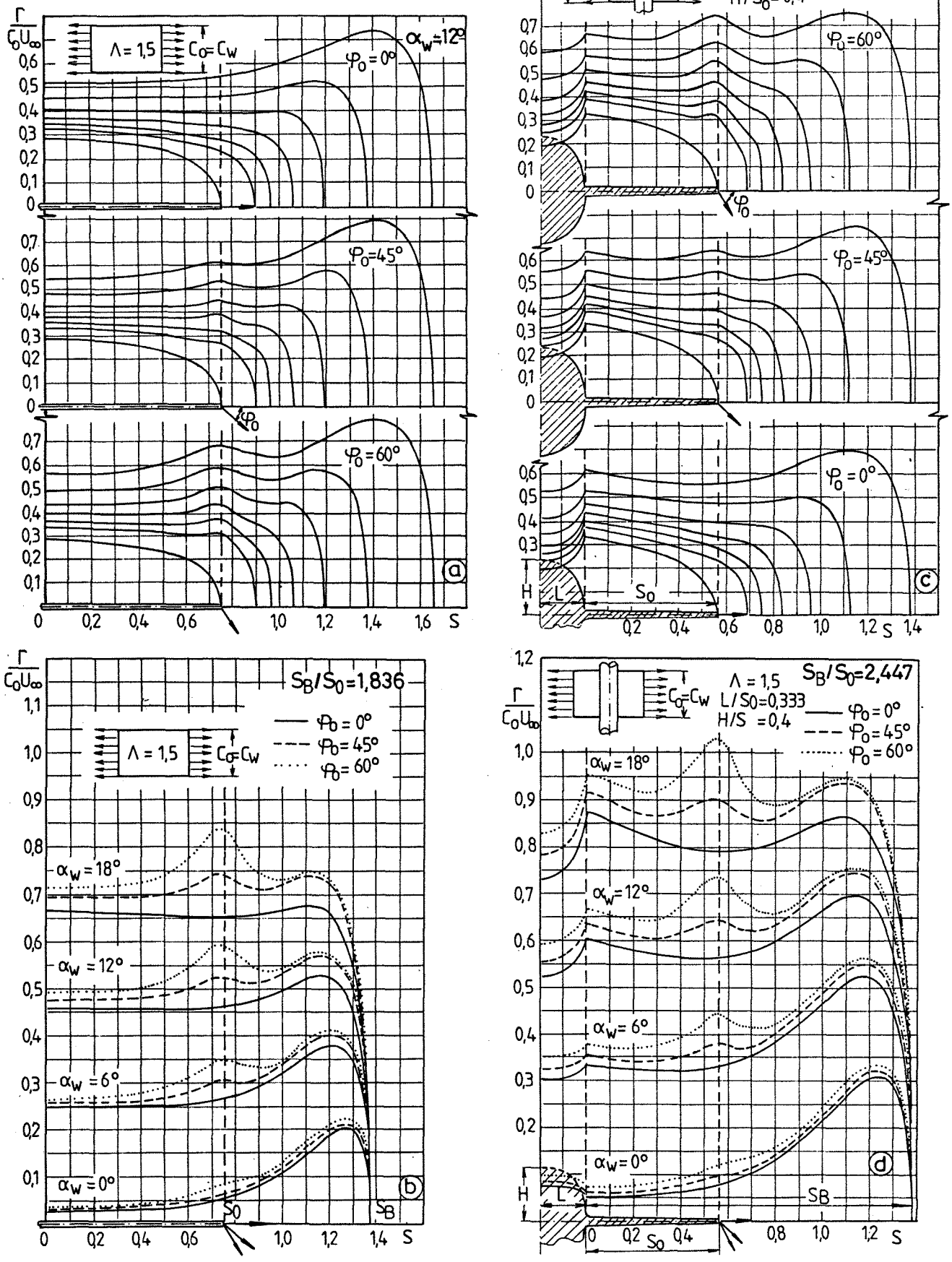

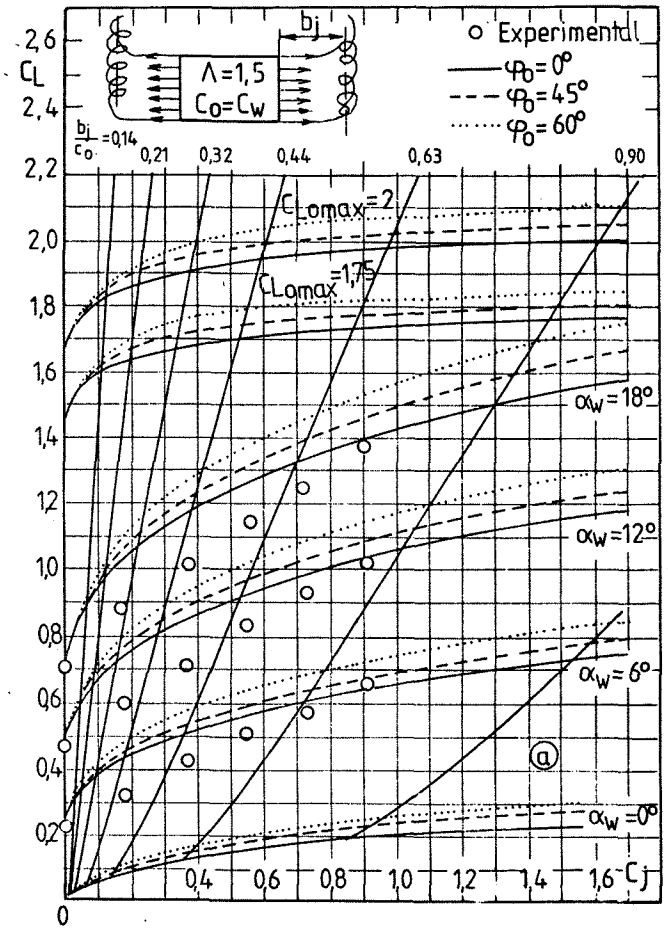

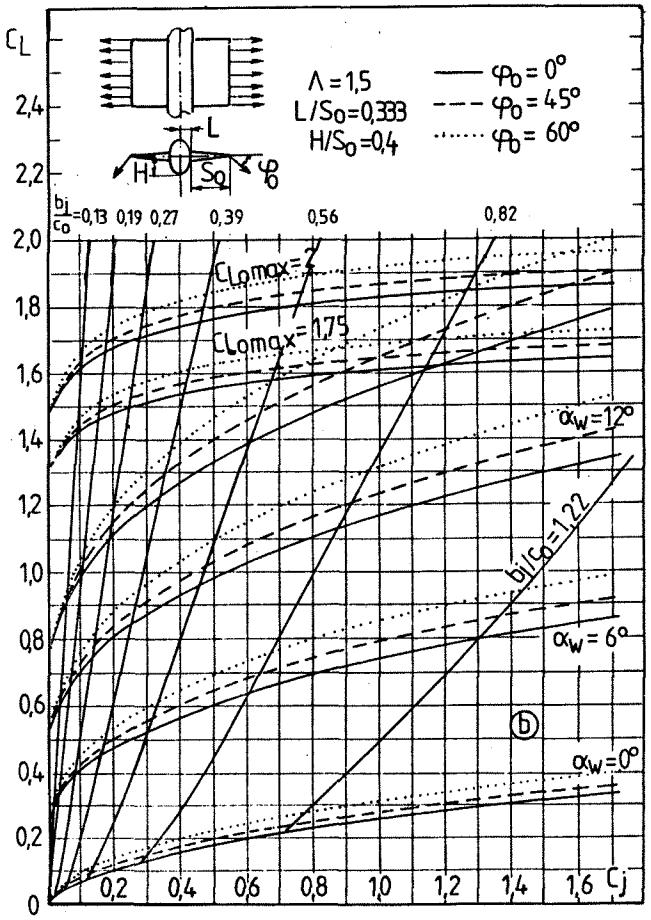

Fig.8a, b Lift increase due to lateral blowing (C_L versus C_j)

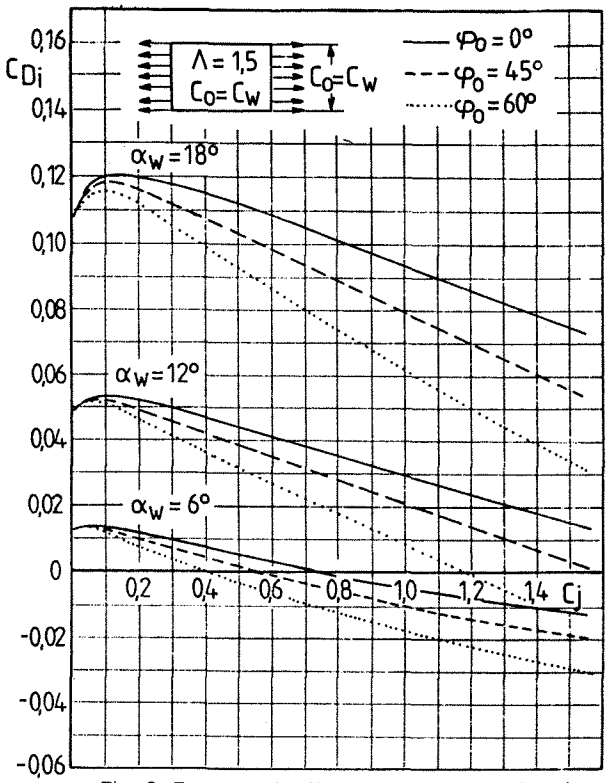

Fig. 9 Drag reduction due to lateral blowing

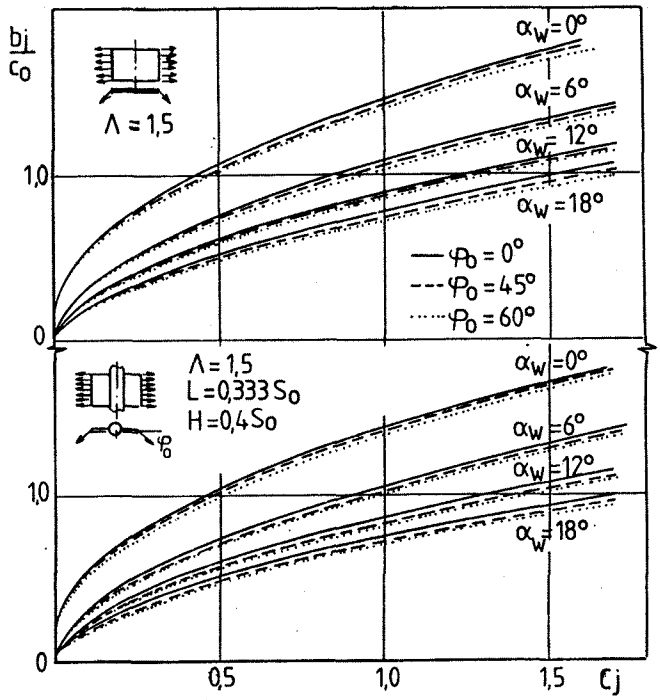

Fig. 10 The lenght of the equivalent jet wing

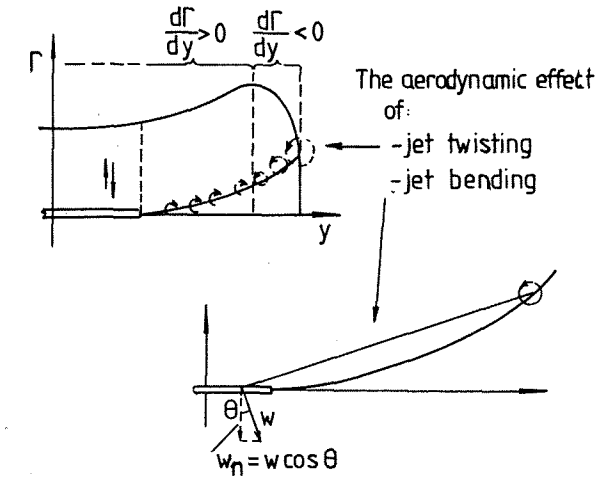

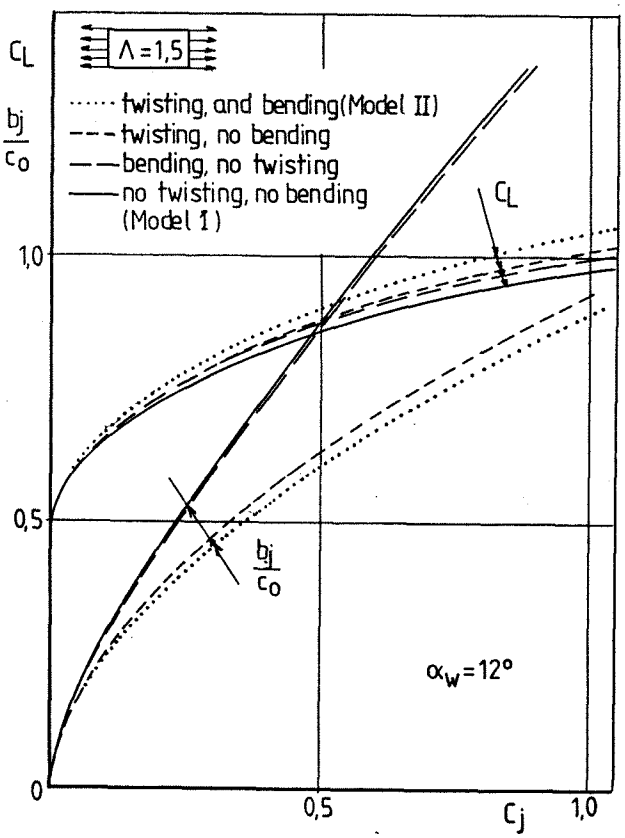

Fig. 11 The influence of the type of equivalent jet wing model (C_L and b_j/c_0 versus C_j)

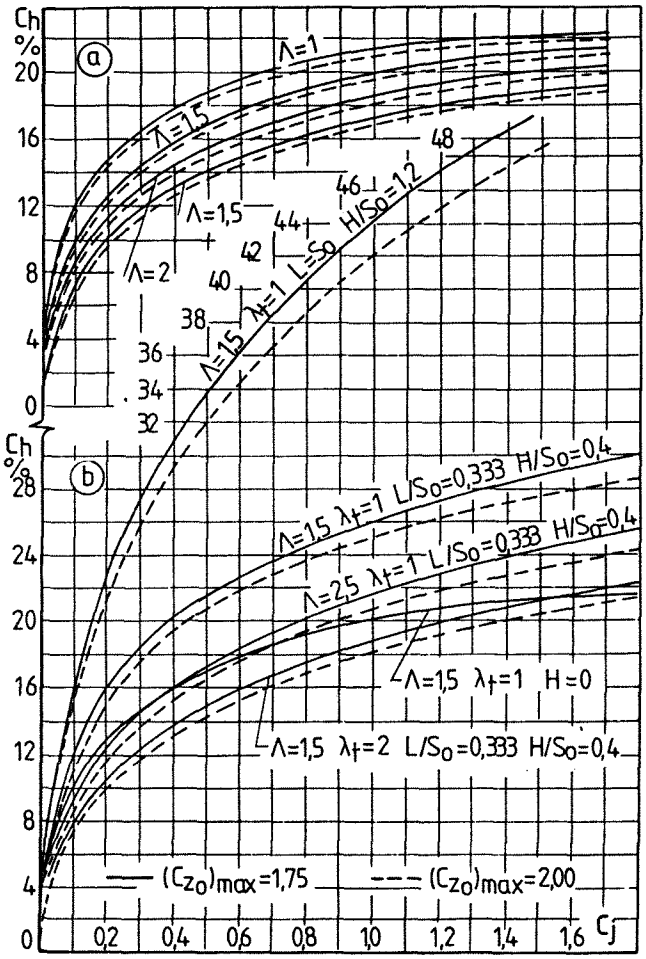

Fig. 12 The maximum lift gain due to lateral blowing for the condition in fig. 5